

Kinetics of Thermal Decomposition Of Aluminum Hydride In Argon¹

Ismail M. K. Ismail* and Tom W. Hawkins
ERC, Inc. at Air Force Research Laboratory/PRSP,
Edwards Air Force Base, CA 93523-7689
Ismail.ismail@edwards.af.mil

ABSTRACT

Thermogravimetric analysis was utilized to investigate the decomposition kinetics of alane (AlH₃) in argon atmosphere and to shed light on the mechanism of alane decomposition. Two kinetic models have been successfully developed and used to propose a mechanism for the complete decomposition of alane and to predict its shelf-life during storage. Under non-isothermal heating, alane decomposes in two steps; the slowest is solely controlled by solid state nucleation of aluminum crystals; the fastest is due to growth of the crystals. Thus, during decomposition, hydrogen gas is liberated and the initial polyhedra AlH₃ crystals yield final amorphous aluminum particles. Nucleation of aluminum atoms is the rate determining step. After establishing the kinetic model, prediction calculations indicated that alane can be stored in inert atmosphere at temperatures below 10°C for long periods of time (e.g. 15 years) without significant decomposition. After 15 years storage, the kinetic model predicts ~ 0.1% decomposition. Storage at higher temperatures (e.g. 30°C) is not recommended.

INTRODUCTION

Recently, the interest in alane (AlH₃) as a solid rocket fuel has been renewed presumably after the development of new methods of preparations and the discovery of new stabilizers that can slow the rate of alane decomposition and thus increase its shelf-life. With the concern on alane thermal stability, extensive physical and chemical characterization of newly produced alane is needed, especially in the area of thermal stability and hydrogen generation during long term storage. Alane can be produced in at least six different crystal forms [1]. The most stable form is α -alane which has been used in the current investigation. The crystals of the α -phase were mostly hexagonal and cubical. Traditionally, the stability of alane is determined by performing a vacuum thermal stability (VTS) experiments [1,2], utilizing the Taliani method [3].

The heat of decomposition of aluminum hydride samples have been measured experimentally in nitrogen atmosphere using a modified bomb calorimeter accommodating a small suspended heating oven containing the sample [4]. At 298 K, the calculated average enthalpy of formation was -11.4 ± 0.8 kJ/mol, absolute entropy was 30.0 ± 0.4 kJ/mol °C and Gibbs energy of formation was 45.4 ± 1.0 kJ/mol. These values indicate that alane is an unstable compound with respect to its forming elements. Thus, thermodynamically, alane should naturally decompose to yield aluminum metal and hydrogen gas.

The kinetics and mechanism of the thermal decomposition of several solvated aluminum hydride compounds have been reported by Zakharov and Tskhai [5]. The volume of decomposition products was traced as a function of time at several isothermal temperatures between 50 and 100°C. For dry alane samples (that is, after the removal of the solvents), an s-shaped type plot was obtained during the liberation of hydrogen. The kinetics of hydrogen liberation was described by a first order autocatalytic equation. The activation energy of this step was 72.2 ± 2.5 kJ/mol. The thermal decomposition of AlH₃ and AlD₃ was investigated using NMR [6]. Samples of alane were decomposed isothermally (at 86-127°C) and typical s-shaped plots, correlating percent decomposition (or amount of aluminum

¹ Approved for public release; distribution unlimited.

Report Documentation Page

Form Approved
OMB No. 0704-0188

Public reporting burden for the collection of information is estimated to average 1 hour per response, including the time for reviewing instructions, searching existing data sources, gathering and maintaining the data needed, and completing and reviewing the collection of information. Send comments regarding this burden estimate or any other aspect of this collection of information, including suggestions for reducing this burden, to Washington Headquarters Services, Directorate for Information Operations and Reports, 1215 Jefferson Davis Highway, Suite 1204, Arlington VA 22202-4302. Respondents should be aware that notwithstanding any other provision of law, no person shall be subject to a penalty for failing to comply with a collection of information if it does not display a currently valid OMB control number.

1. REPORT DATE MAY 2005	2. REPORT TYPE	3. DATES COVERED -			
4. TITLE AND SUBTITLE Kinetics of Thermal Decomposition of Aluminum Hydride in Argon (Technical Paper)		5a. CONTRACT NUMBER			
		5b. GRANT NUMBER			
		5c. PROGRAM ELEMENT NUMBER			
6. AUTHOR(S) Ismail Ismail; Tom Hawkins		5d. PROJECT NUMBER 5026			
		5e. TASK NUMBER 0541			
		5f. WORK UNIT NUMBER			
7. PERFORMING ORGANIZATION NAME(S) AND ADDRESS(ES) Air Force Research Laboratory (AFMC), AFRL/PRSP, 10 E. Saturn Blvd., Edwards AFB, CA, 93524-7680		8. PERFORMING ORGANIZATION REPORT NUMBER			
9. SPONSORING/MONITORING AGENCY NAME(S) AND ADDRESS(ES)		10. SPONSOR/MONITOR'S ACRONYM(S)			
		11. SPONSOR/MONITOR'S REPORT NUMBER(S)			
12. DISTRIBUTION/AVAILABILITY STATEMENT Approved for public release; distribution unlimited					
13. SUPPLEMENTARY NOTES					
14. ABSTRACT Thermogravimetric analysis was utilized to investigate the decomposition kinetics of alane (AlH₃) in argon atmosphere and to shed light on the mechanism of alane decomposition. Two kinetic models have been successfully developed and used to propose a mechanism for the complete decomposition of alane and to predict its shelf-life during storage. Under non-isothermal heating, alane decomposes in two steps; the slowest is solely controlled by solid state nucleation of aluminum crystals; the fastest is due to growth of the crystals. Thus, during decomposition, hydrogen gas is liberated and the initial polyhedra AlH₃ crystals yield final amorphous aluminum particles. Nucleation of aluminum atoms is the rate determining step. After establishing the kinetic model, prediction calculations indicated that alane can be stored in inert atmosphere at temperatures below 10°C for long periods of time (e.g. 15 years) without significant decomposition. After 15 years storage, the kinetic model predicts ~ 0.1% decomposition. Storage at higher temperatures (e.g. 30°C) is not recommended.					
15. SUBJECT TERMS					
16. SECURITY CLASSIFICATION OF:			17. LIMITATION OF ABSTRACT	18. NUMBER OF PAGES 10	19a. NAME OF RESPONSIBLE PERSON
a. REPORT unclassified	b. ABSTRACT unclassified	c. THIS PAGE unclassified			

produced) versus reaction time, t , were obtained. Each s-curve was divided into three regions; the first of which corresponded to an induction period, τ_{ind} , where the rate constant $k_1 = 1/\tau_{\text{ind}}$. The value of τ_{ind} was defined as the time taken to achieve 5% decomposition (or when the fraction of original alane converted to aluminum, α is 0.05). In the second region, an “acceleration period” [6] was noted between $\alpha = 0.1$ and 0.6; the equation governing the kinetics in this region was $\alpha^{1/3} = k_2 t$. The third region, $\alpha = 0.6 - 0.9$, was defined as the deceleration region, the kinetic rate was controlled by a third equation: $\ln(1-\alpha)^{-1} = k_3 t$. The activation energies for the three regions were 97, 108 and 112 kJ/mol, respectively, within an error of 20% [6]. A comparison between decomposition kinetics of AlH_3 and AlD_3 showed that the deuteride was decomposing at a slower rate than the hydride. For example, at 107°C, the induction period for the deuteride was 5 times longer than that of the hydride, and the rate constant for the deuteride (presumably in the second region) was half of that for the hydride [6]. The differences were attributed to the presence of different impurities and crystal defects in each sample and also to differences in particle size. The effect of particle size of the hydride at 107°C was studied between 50 and 150 μ , decomposition kinetics were highly dependent on particle size [6]. For example, to achieve the complete liberation of hydrogen, it took ~ 350 min for the sizes $> 150 \mu$ but only ~ 90 min for the 50 μ particles. The implication of this is that the thermal stability of alane can be enhanced, to a point, simply by increasing the starting particle size of alane.

Over the past decade, significant improvement was made to produce kinetic modeling software that help investigators to better understand the kinetics and mechanism of chemical reactions [7-19]. These programs proved to be useful in many applications. Typical commercial software are available such as “Model Free Kinetics” by METTLER or “Thermokinetics” by NETZSCH (which was used for the work cited in this article) and AKTS-TA-Software. The Thermokinetics program has several mathematical models that prescribe chemical reactions and solid state transformations. The models include n^{th} order reactions, Avrami-Erofeev solid state transformation [20] and autocatalytic reactions. A single one-step model or a combination of models (more than one step reaction) can be chosen for performing the analysis. These software programs have been used in the recent literature to investigate the thermal decomposition of many energetic materials [10-17], of hazardous materials during storage [18] and the thermal reactions of rocket motor propellants [19]. To our knowledge, a similar investigation on kinetics of alane decomposition has not been reported in the open literature.

The objectives of the present work were to develop kinetic equations that can accurately describe the decomposition process of alane in an inert atmosphere, to use the model and propose a mechanism for alane decomposition and to use the model and predict the storage life of alane at ambient conditions.

EXPERIMENTAL

The alane samples used in the present investigation had the following elemental analysis: average weight percentage of aluminum was 88.26%, of hydrogen 9.96% and of carbon 0.44%. The balance, obtained by difference, 1.54% was assigned to oxygen.

A Mettler TGA unit (model SDTA-851e) was used with Mettler proprietary software STAR^e version 8.0. Ultra-high-purity argon (UHP certified purity: 99.9999% Ar) was passed through the samples at a flow rate of 60 cc/min. Before starting a test, a sample was placed in a quartz container, flushed with argon for 20 minutes and finally heated at a projected constant heating rate, between 0.5 and 20 C/min from room temperature to 350°C. After terminating a run, the density of residue was determined using a Micromeritics helium micro-Accu-Pycnometer (cell volume: 0.25 cc and expansion volume: 0.73 cc). For the TGA data, the decomposition of alane was evaluated using NETZSCH-Thermokinetics software supplied by NETZSCH-Gerätebau GmbH in Germany.

The surface area and porosity development of one alane sample was studied in the following manner, using an automated surface area apparatus, Digisorb 2600, manufactured by Micromeritics

Instrument Corporation. Successive runs were performed on the sample while alternating between a pre-evacuation step at 60°C for a selected length of time, and actual measurements of surface area using krypton adsorption at -196°C. The sample was always kept under vacuum, in He or Kr without ever being exposed to ambient air for the entire set of tests. This practice insured that the generated aluminum did not oxidize during the measurements. Specific surface area, SA (m²/g), was calculated from Kr adsorption isotherms using the BET equation. The cross-sectional area of a Kr atom adsorbed at the surface was taken as 0.210 nm²/Kr atom [21].

RESULTS AND DISCUSSION

SEM examination showed that alane particles are mostly cubes with fewer pentagonal and hexagonal crystal shapes. Occasionally, cracks and pits are noted on the surface but these are not deep. The SEM size of the particles ranges between 3 and 20 μ. The surface area of as-received alane was 0.215 m²/g. This value is small and suggests that alane particles are non-porous or, at least, have insignificant level of porosity. Assuming that all particles are cubical, the average size of particles, and the equivalent length of their sides, L (in microns), can be estimated using: $L = 6 / (\text{surface area} \times \text{density})$. The average value of L is 18.8 μ which is within the SEM size range.

Theoretically, when alane completely decomposes to yield aluminum, the density increases from 1.486 to 2.71 g/cc. These values were confirmed in the present investigation on the starting alane and on the final products, using helium pycnometry. From the published crystallography data, the crystal size and structure should also be changing from hexagonal alane (lattice parameters: a = 0.54 nm and c = 1.14 nm) [22] to face centered cube (FCC) aluminum (a = 0.404 nm). Between these two extremes, one would expect a combination of the two structures with the alane crystals breaking down and the growth of aluminum crystals. To shed more light on this effect, the following series of surface area measurements were performed. A fresh alane sample was evacuated at room temperature for 24 h; it lost 2.28%. The first Kr-surface area measurement was measured: 0.215 m²/g. The sample was evacuated again at room temperature for additional 24 h, there was no further weight loss, and the surface area remained the same. The sample was again evacuated for additional 72 h. Again, there was no weight loss or change in surface area. This means that the 2.28% loss after the first evacuation was due to evolution of moisture, solvent (if any) and other volatiles adhering to particle external surfaces.

The sample was then evacuated stepwise at 60°C for successive periods of time. After each evacuation, the sample was kept under a blanket of ultra high purity He to avoid possible contamination with air and to eliminate the possibility of oxidizing the fresh nascent aluminum active sites developed during hydrogen liberation. After each He fill up, the sample was weighed and a Kr surface area measurement was executed. These two consecutive steps were repeated several times until the final sample weight became constant; corresponding to the complete decomposition of alane. That is, the remaining weight was ~ 90% of the starting weight. The results are displayed in Figure 1. The plot has three main regions. In the first region, between 0 and 1.9% weight loss, the surface area is essentially the same. In this region there is probably loss of hydrogen atoms attached to the external surface of alane cubes plus those attached to the internal walls of open cracks, pits and crevices. The alane particles in this region are, most likely, intact; their sizes are essentially the same as the starting alane. In the second region, between ~ 2 and 7.5% weight loss, the particles develop porosity as a result of the excessive hydrogen gas pressure exerted on pore walls. The walls begin cracking, the pores begin opening and the original crystal structure is opened. As more pores continue to open, the surface area keeps increasing until a maximum is reached at ~ 7.5% weight loss. In the third region, the surface area drops abruptly to ~ 0.35 m²/g and remains constant at this value. This suggests that the final cubical structure of aluminum produced may only dominate after 75% of the original hydrogen evolves.

The ratio between the final specific surface area of Al and starting surface area of alane was approximately 1.63. This increase is attributed to two main reasons: a decrease in particle size after

decomposition and an increase in surface roughness. The surfaces of partially and fully decomposed alane samples are shown in Figure 2. Plate (a) shows that the particles have developed pores and cracks after 3.1% weight loss, and that the external surface acquired slight roughness. Plate (b) shows the surface after the complete decomposition of alane, the roughness has increased drastically and there are small debris of (probably) aluminum metal covering the surface. The average particle size, for the larger particles in the completely decomposed sample, is the range of 12-16 μ , compared to 18-20 μ for the starting alane. The experimental density of final residue after complete decomposition (plate b) was 2.69 g/cc which is close to the theoretical value of 2.71 for pure aluminum.

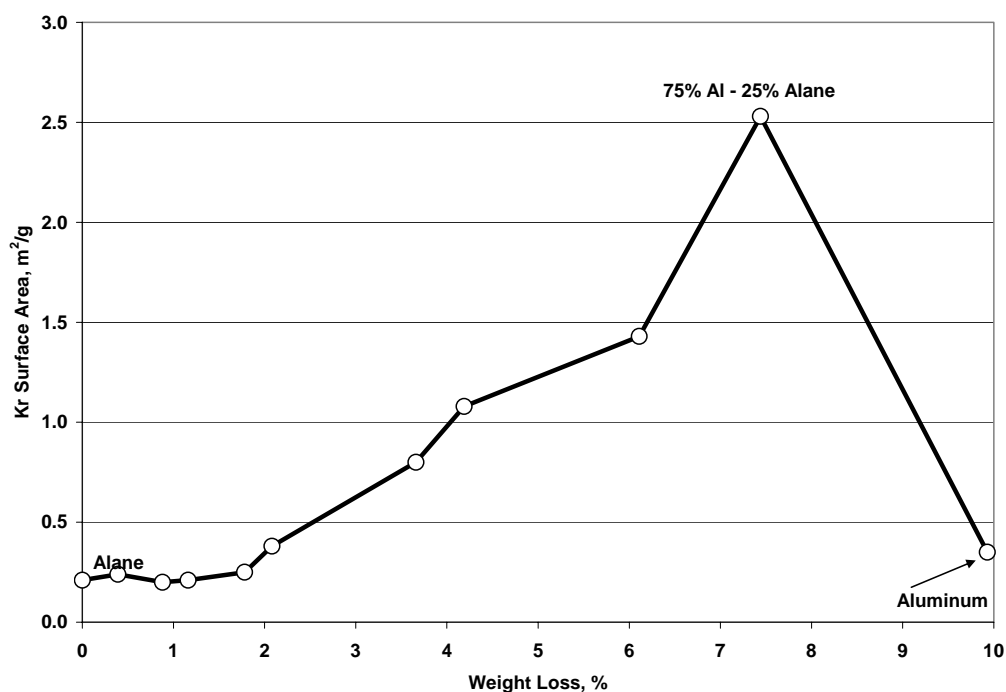


Figure 1. Dependence of surface area of alane on extent of hydrogen evolution.

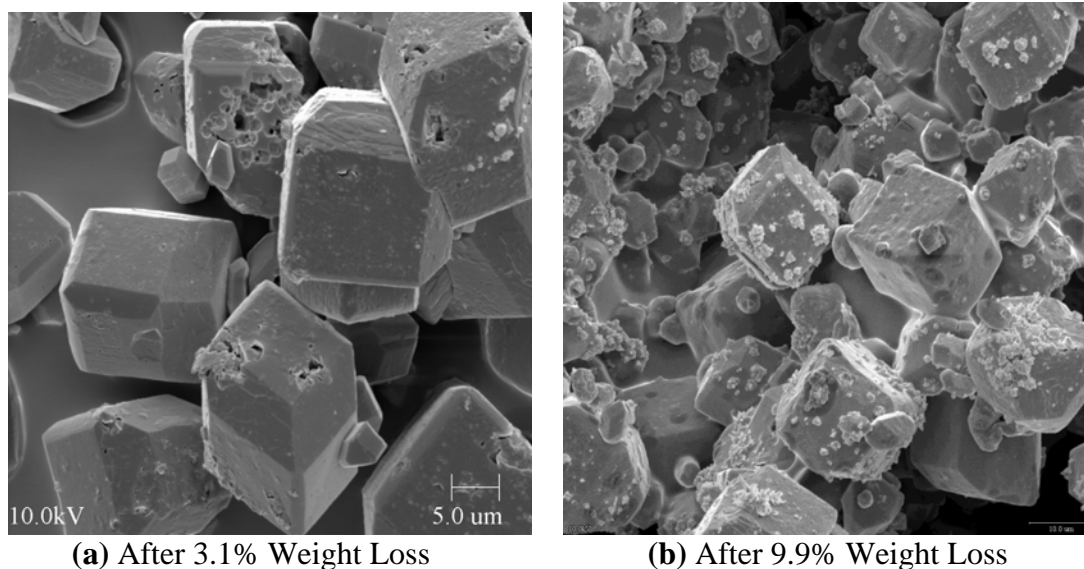


Figure 2. SEM photos for (a) partially decomposed alane (3.1% weight loss) and (b) completely decomposed alane

The TGA results for alane decomposition in Ar at six heating rates (0.49, 0.98, 2.0, 4.9, 9.9 and 20.2°C/min) are shown in Figure 3. At 20.2°C/min, the decomposition began at 180°C and was completed at 215°C; the final weight loss was 9.9%; indicating that the hydrogen content of alane was completely removed. For the three repeated runs performed at 9.9°C/min, the reproducibility of the data was quite satisfactory and the average weight loss was 9.05%. The decomposition began at a lower temperature (168°C) and was completed at 197°C. This trend continued with the other heating rates. The main noticeable trend is that as the heating rate decreased, the final weight loss became smaller. That is, a sample with a low heating rate retained more hydrogen than another one decomposing at a higher heating rate. It appears that when alane decomposes at a lower heating rate, the porous structure closes earlier and a portion of the hydrogen stays trapped inside the particles. Also, at a lower heating rate, decomposition occurs at lower temperatures; the diffusion of hydrogen through the particles or the nucleation of aluminum sites is slow.

To perform kinetic analysis, we have pursued two independent approaches: the classical “model free kinetics” (MFK), and a more precise curve-fitting thermo-kinetics modeling (TKM) analysis. The classical MFK approach was used first to evaluate the activation energy and the pre-exponential factor. Based on the findings with MFK, the more sophisticated TKM approach is then used with as many necessary intermediate kinetic steps and reaction orders as needed to mathematically describe the steps involved. The model showing the lowest possible standard deviation was assigned to the decomposition reaction. Finally, a physical model for the overall reaction is proposed.

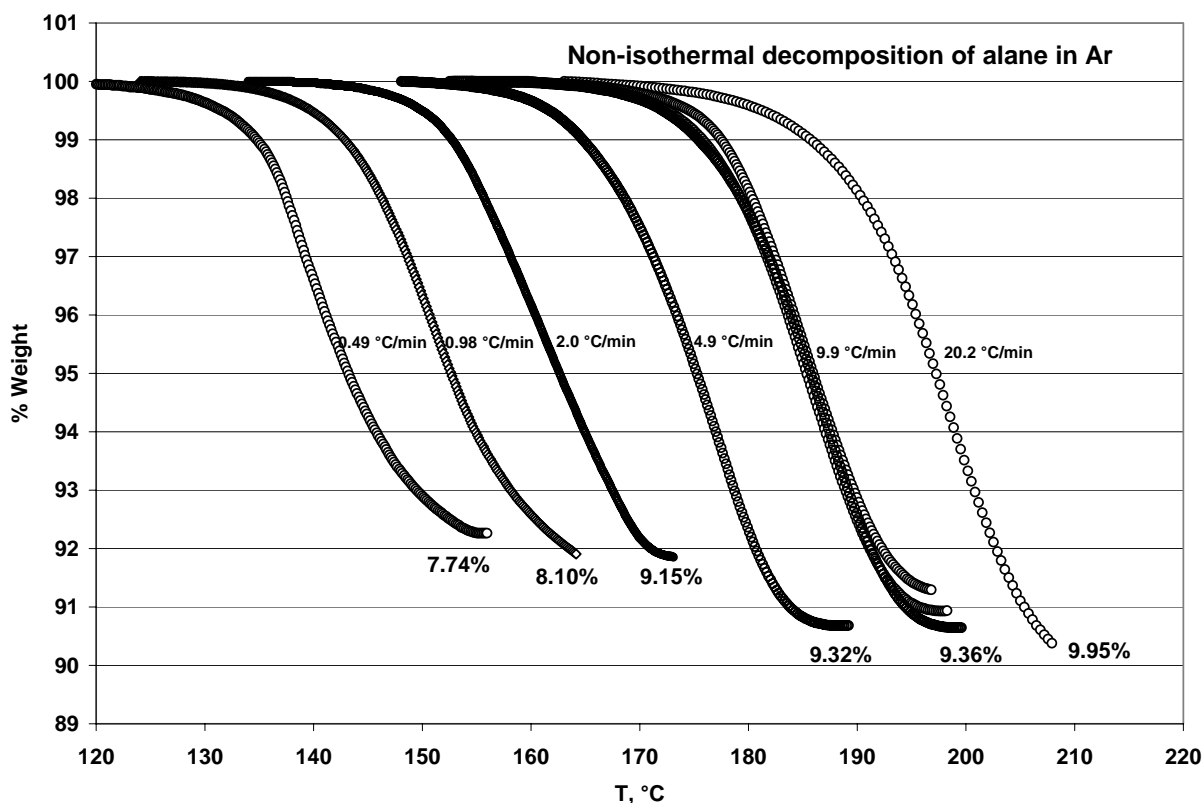


Figure 3. Decomposition of alane in Ar (50 cc/min) at different heating rates.

The classical MFK computations include three main well-established approaches: the ASTM method [23], the Friedman analysis [24], and the Ozawa-Flynn-Wall analysis [25,26]. With each

approach, the activation energy, E_a , and the pre-exponential term, A are calculated. Figure 4 illustrates the ASTM analysis for alane decomposition: $E_a = 97.0 \pm 3.1$ kJ/mol and $A = 2.04 \times 10^{-8}$ s $^{-1}$.

The second MFK method is the Friedman analysis [24] which is based on the iso-conversion method: at a given level of decomposition or conversion, α , the instantaneous decomposition rate and its corresponding temperature are calculated at each heating rate. This step is repeated at other levels until the reaction is completed ($\alpha = 1$). Values of E_a , and A are calculated at different values of α . The results, which are summarized in Figure 5, suggest that alane decomposition follows, at least, two steps: the first starts and continues up to ~ 0.25 conversion and the second occurs between 0.25 and 0.85 conversion. This finding is in line with the results of specific surface area reported above (Figure 1).

The third MFK method is the Ozawa-Flynn-Wall analysis [25,26] which also utilizes the iso-conversion approach. The results are shown in figure 5 suggesting that the activation energy of alane decomposition is constant through the entire reaction with an average value of 103 ± 3 kJ/mol. In this case, the decomposition of alane would follow first order kinetics. This is not the case. Attempts were made to fit the original raw data to a simple first order decomposition kinetics involving the decomposition reaction of: Alane \rightarrow Aluminum + H $_2$. The rate of this reaction would be given by: $(d\alpha/dt) = A * (1-\alpha) * \exp(-E_a/RT)$, where R is the gas constant. As shown in Figure 6 (dotted lines), alane decomposition does not follow first order kinetics.

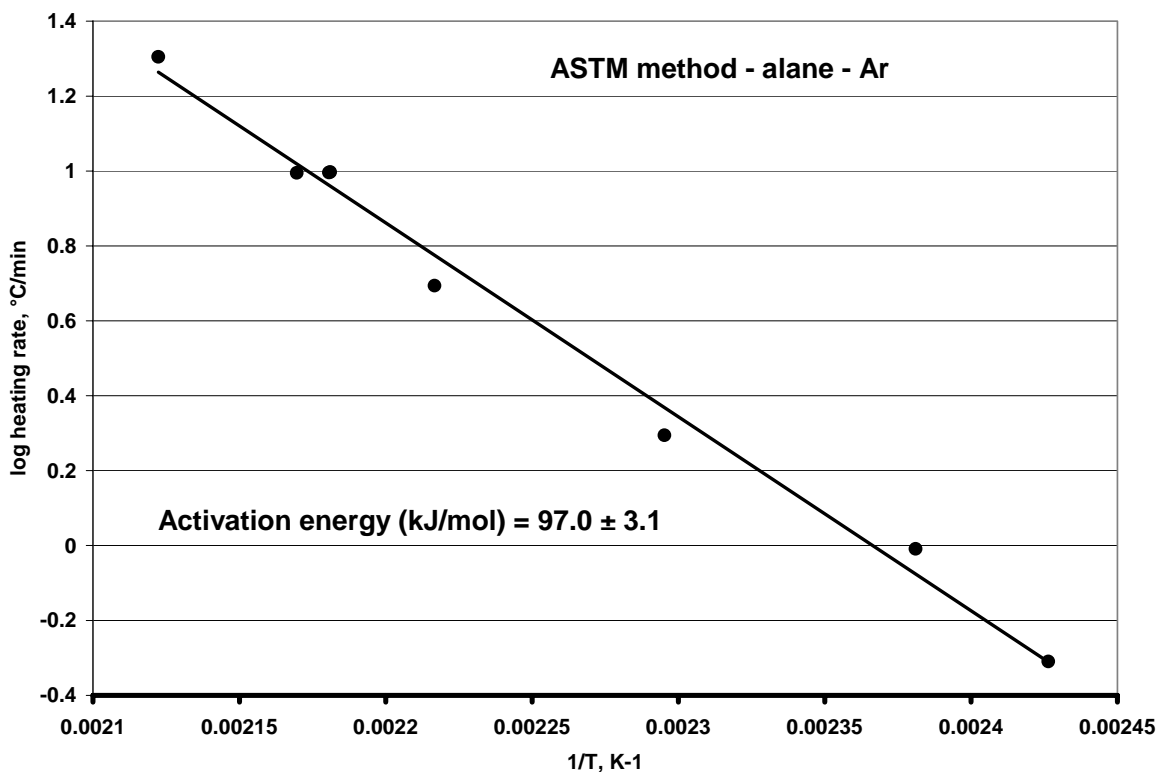


Figure 4. Arrhenius plot for decomposition of alane in Ar using the ASTM method.

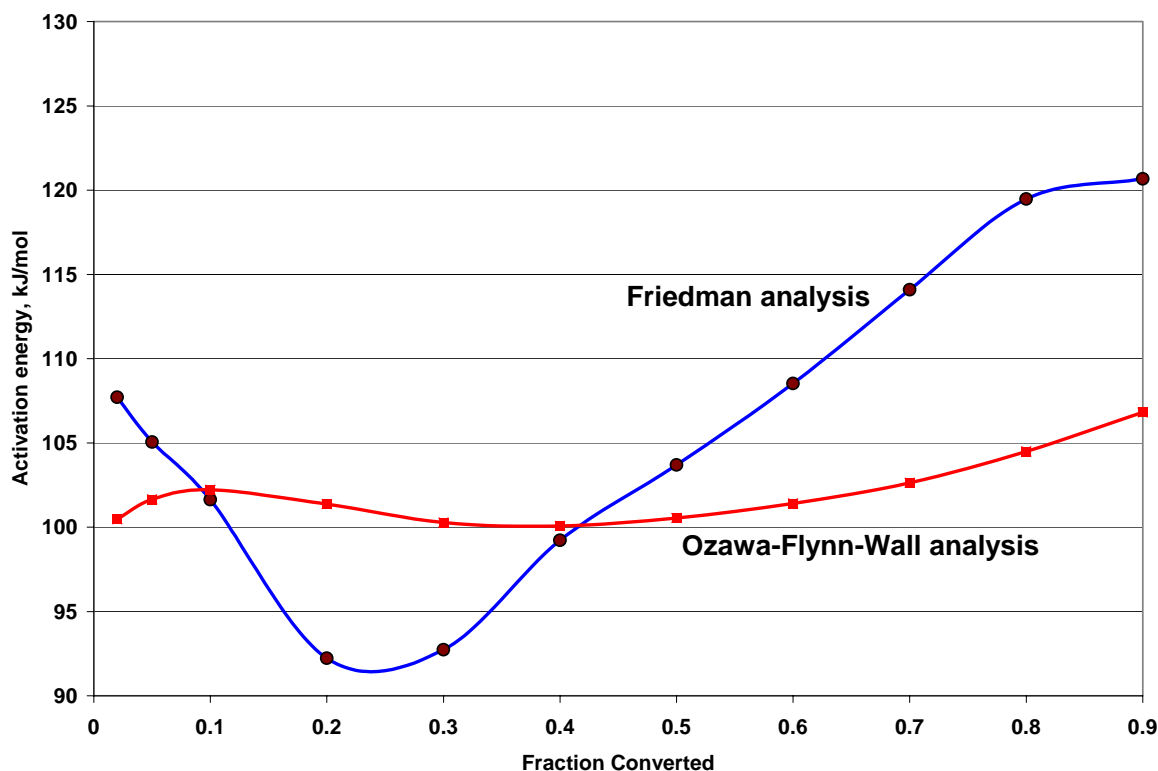


Figure 5. Variation of activation energy with level of alane conversion to yield aluminum.

Subsequently, more complicated two-step kinetic models were considered; the most promising included two-step consecutive reactions of the type: $A \rightarrow B \rightarrow C$. The two best fitting models have been chosen, they are referred to here as Model-A and Model-B. Both models were statistically near perfection with correlation coefficients better than 0.998. In both cases, step-1 ($A \rightarrow B$) was basically the same; it was governed by the Kolmogorov-Johnson-Mehl-Avrami (KJMA) equation (a modified Avrami equation), which describes mainly an n^{th} -dimensional nucleation or growth reaction [20, 27-29]. The KJMA model has been represented recently by the following equation proposed by Nakamura [29]:

$$d\alpha/dt = n * k(T) * (1 - \alpha) * [-\text{Ln}(1 - \alpha)]^{(n-1)/n}$$

where $k(T)$ is the rate constant, given by: $k(T) = A * \text{Exp}(-E/RT)$. Here A is the pre-exponential factor and E is its activation energy. The Avrami exponent, n , is normally used as a tracer for the dimensionality of the reaction. Commonly accepted guidelines state that for one-dimensional growth, $n \leq 2$; for two-dimensional growth, $n = 2 - 3$ and for 3 dimensional growth, $n = 3 - 4$ [29, 30]. Values of the kinetic parameters obtained here for step-1 in Model-A and Model-B are listed in Table 1.

The second steps for Model-A and Model-B can be equally described statistically by two different equations. For Model A, step-2, satisfied, once again, a second KJMA equation; the parameters of which are displayed in Table 1; they are lower than those of step-1. However for Model-B, the kinetics satisfied a typical chemical reaction kinetics (with n^{th} order kinetics) of the type: $d\alpha/dt = A_2 * (1-\alpha)^n * \text{Exp}(-E_2/RT)$. In this case, the order of the reaction (power of the conversion term) was 2.52. The two models gave excellent fitting to the raw data as indicated by the solid lines shown in Figure 6 (Because the fitting is excellent, it may be hard to see the complete solid lines at certain regions of the plots since the solid lines are perfectly superimposing the raw data points). From the statistical

analysis, correlation coefficients and standard deviation values, Model-A appeared slightly better than Model-B. However, Model-B could not be ruled out because its fitting to the data was also excellent.

Based on Model-A, step-1 has a higher activation energy, pre-exponential term and Avrami exponent than Step-2 (Table 1). The Avrami exponent, n_1 is between 2 and 3 which suggests that the first step for alane decomposition is a two-dimensional nucleation reaction (possibly) taking place at the outer surface of the particles (two dimensional nucleation).

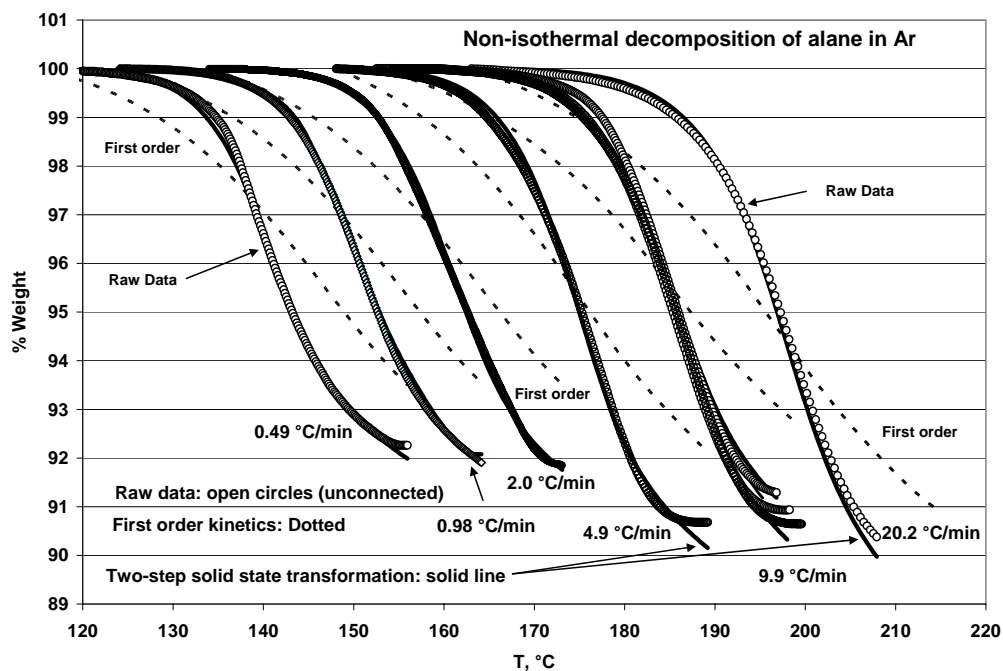


Figure 6. Comparison between the experimental data of alane decomposition (open circles), first order decomposition kinetics model (dotted lines) and two-step reaction model (solid-line).

Table 1: Calculated kinetic parameters for non-isothermal decomposition of alane in argon.

	Model-A	Model B
<i>Step-1</i>		
A_1, s^{-1}	$5.61 * 10^7$	$9.18 * 10^8$
$E_1, kJ/mol$	83.8	99.0
Avrami exponent: n_1	2.23	2.43
<i>Step-2</i>		
A_2, s^{-1}	$4.92 * 10^5$	$3.08 * 10^9$
$E_2, kJ/mol$	63.1	88.5
Avrami exponent: n_2	0.63	N/A
reaction order	N/A	2.52

For Model-A, step 2 has lower values of A, E and n than step-1. The rates for this step are much faster than in step-1. This step is attributed to a growth reaction; the growth of aluminum layers on the nucleation sites already developed in step-1. The small value of n_2 , which is < 1 , suggests that the growth reaction is a one-dimensional process, most likely, starting at the outer surface of the particles and continuing inwards towards their center.

As mentioned earlier, with Model-B, step-1 was similar to that of Model-A, however, step-2 was not the same; it followed a simple rate law expression of the type: $d\alpha/dt \sim (1 - \alpha)^n$, where n (value = 2.52) is the overall order of the second step. One possible explanation is that the aluminum atoms, once formed after step-1, may move over the surface and collide with each other to form metallic bonds or amorphous structure. With this assumption, the aluminum atoms have to collide with each other at a rate of 2 -3 times, on the average, before they bond to each other. If this is the case, the number of collisions at the beginning of growth process would be high (say 3 or 4) and it will decrease, due to the proximity of aluminum atoms, as the growth process continues. Further qualification for this mechanism is beyond the scope of this article and is left to future research.

With the two models developed, the prediction of alane shelf-life during storage at 5, 10, 15, 20, 25 or 30°C was computed. The results, which are displayed in Table 2, show two significant trends. First, Model-A predicts longer shelf-life than Model-B. For example, after 3 years storage at 20°C, while Model-A predicts 0.13% weight loss of hydrogen, however, Model-B predicts 1.02% weight loss. It is recalled that the sample had 9.95% elemental hydrogen content which is smaller than the theoretical value of 10.08% by 0.13%. Since this sample has been stored in our laboratories at ambient temperature for ~ 3 years, one concludes that Model-A appears more realistic for predictions than Model-B. Second, the prediction shows clearly how sensitive alane decomposition is to storage temperature fluctuations. For example, if alane is stored for 10 years at 5-10°C, the amount decomposed (as per Model-A) is insignificant; at 15°C the sample loses 0.31% and at 30°C it loses most of its hydrogen (8.61%). Thus, the important critical element to extend the shelf life of alane is to store it at low temperatures, preferably in the neighborhood of 10°C.

Table 2: Prediction of weight percent of hydrogen evolved during storage of alane

(a) Model-A							(b) Model-B						
Years	5°C	10°C	15°C	20°C	25°C	30°C	Years	5°C	10°C	15°C	20°C	25°C	30°C
1	0.00	0.00	0.01	0.03	0.08	0.28	1	0.00	0.01	0.03	0.10	0.42	1.74
3	0.00	0.01	0.03	0.13	0.76	3.39	3	0.01	0.05	0.22	1.02	3.52	5.79
5	0.00	0.01	0.07	0.42	2.43	6.37	5	0.03	0.14	0.68	2.76	5.27	7.22
10	0.01	0.04	0.31	2.10	6.27	8.61	10	0.12	0.62	2.67	5.16	7.16	9.02
15	0.02	0.10	0.85	4.29	7.86	9.18	15	0.29	1.47	4.19	6.24	8.28	9.77

CONCLUSIONS AND RECOMMENDATIONS

1. The decomposition of alane starts with hydrogen liberation from external surface and pre-existing pores and cracks. Porosity then increases while the size of alane particles decreases. When the decomposition is completed, the pores are closed in the final product (aluminum).
2. With Freidman MFK analysis, however, alane decomposition involves two steps; this finding is supported by the results of surface area measurements.
3. Alane decomposition can be better described by solid-state transformation kinetics (nucleation and growth mechanism). Two kinetic models have been developed and their fit to the experimental data was confirmed. The models were used to estimate the shelf-life of alane when stored in inert atmospheres for several years.
4. Alane decomposition in Ar involves two major consecutive steps: $A \rightarrow B \rightarrow C$; representing the transformation of hexagonal alane crystals to amorphous aluminum particles. Step-1 is due to a slow nucleation reaction; possibly with the formation of aluminum nucleation sites at the outer surface of the particles. This is the rate determining step for alane decomposition and the kinetics are controlled by an Avrami-type (KJMA) equation. The second step is postulated as the growth of aluminum layer towards the center of the particles (step-2).

5. With Model-A developed, the projected decomposition of alane in 15 years (or less) is very small, ~ 0.1%, if stored below 10°C. Storing alane at higher temperatures is not recommended; the material may lose as much as its entire hydrogen content if stored for 15 years at 30°C.

Acknowledgement

The authors want to thank Dr. Ronald Channell, Dr. Frank Roberto, Dr. Robert Corley, Dr. Keith McFall, Mr. John Clark, Mr. Paul Jones, Dr. George Harting and Dr. Donald Tzeng for their fruitful discussions, suggestions and support. The technical assistance of Ms Marietta Fernandez (SEM examinations) and of Ms Leslie Hudgens (density measurements) is highly appreciated. I. M. K. Ismail is appreciative to late Dr. J. Opfermann for his invaluable advice and the effort he made in modifying the kinetics software to meet our needs.

REFERENCES

1. F. M. Brower, N. E. Matzek, P. F. Reigler, H. W. Rinn, C. B. Roberts, D. L. Schmidt, J. A. Snovar, K. Terada; *J. Am. Chem. Soc.* 98(9) (1976) 2450-2453.
2. G. C. Sinke, L. C. Walker, F. L. Oetting, D. R. Stull; *J. Chem. Phys.* 47 (1967) 2759.
3. M. Taliani; *Gazz. Chim. Ital.* 51 (1921) 184.
4. M. A. Petrie, J. C. Bottaro, R.J. Schmitt, P. E. Penwell, D. C. Bomberger; *United States Patent* US 6228338 B1 (2001).
5. V. V. Zakharov, A. N. Tskhai; *Russian Journal of Inorganic Chemistry* 37 (9) (1992) 997.
6. V. P. Tarasov, Yu. B. Muravve, S. I. Bakum, A. V. Novikov; *Doklady Phys. Chem.* 393 (2003) 4.
7. S. V. Vyazovkin, A. I. Lesnikovich ; *Thermochimica Acta* 165 (1990) 273-280.
8. S. Vyazovkin, V. Goryachko; *Thermochimica Acta* 194 (1992) 221-230.
9. S. Vyazovkin, C. A. Wight; *Ann. Rev. Phys. Chem.* 48 (1997) 125-149.
10. J. Opfermann, W. Haedrich; *Thermochimica Acta* 263 (1995) 29 – 50.
11. S. Vyazovkin, C. A. Wight; *Thermochimica Acta* (1999) 340-341 53-68.
12. S. Vyazovkin; *Int. Rev. Phys. Chem.* 19 (2000) 45-60.
13. S. Vyazovkin, C. A. Wight; *Chem. Mater* 11 (1999) 3386-3393.
14. S. Vyazovkin, J. S. Clawson, C. A. Wight; *Chem. Mater.* 13 (2001) 960-966.
15. S. Vyazovkin, C. A. Wight; *J. Phys. Chem. A* 101 (1997) 8279-8284.
16. S. Vyazovkin, C. A. Wight; *J. Phys. Chem. A* 101 (1997) 5653-5658.
17. H. J. Flammersheim, J. Opfermann.; *Thermochimica Acta* 337 (1999) 149-153.
18. J. Opfermann, W. Haedrich; *Thermochimica Acta* 263 (1995) 29 – 50.
19. B. Roduit, C. Borgeat, B. Berger, P. Folly, B. Alonso, J.N. Aebischer; *Proceedings of the 31st International Pyrotechnics Seminars* (2004) 11-16 July, Fort Collins, Colorado, USA.
20. M. Avrami; *J. Chem. Phys.* 7 (1933) 1103-1112, 8 (1939) 212-224, 9 (1940) 177-184.
21. I. M. K. Ismail; *Langmuir* 8 (1992), 360.
22. Turley, J. W and Rinn, H. W; *Inorg. Chem.* 8 (1969) 18.
23. H. E. Kissinger; *J. Res. Nat. Bur. Stds* 57 (1956) 217.
24. H. L. Friedman; *J. Polymer Lett.* 4, (1966) 323.
25. T. Ozawa; *Bull. Chem.Soc., Japan* 38, (1965) 1881.
26. J. Flynn, L. A. Wall; *Polymer Lett.* 4, (1966) 232.
27. A. N. Kolmogorov; *Izvestiya Acad. Nauk SSSR, Ser. Math.* 1 (1937) 355.
28. W. A. Johnson, P. A. Mehl; *Trans. Am. Inst. Mining Metall. Eng* 135 (1939) 416.
29. N. Nakamura, K. Katayama, T. Amano; *J. Appl. Polym. Sci* 17 (1975) 1031.
30. T. Pradell, D. Crespo, N. Clavaguera, M. T. Clavaguera-Mora; *J. Phys. : Condens. Matter* 10 (1998) 3833.